Int J Clin Exp Med 2019;12(7):9446-9452
www.ijcem.com /ISSN:1940-5901/IJCEM0086717

Case Report

Computer-aided design and manufacturing with 3D printing for cranio-orbital defect reconstruction and artificial eye implantation: single case report and literature review

Liuxueying Zhong[1*], Huawei Jin[2*], Dan Chen[3], Bing Shu[2], Haotian Lin[1], Juejing Chen[1], Jingyi Peng[1], Zhenhua Yu[2], Yongxin Zheng[1]

[1]Department of Ocular Trauma, Zhong Shan Ophthalmic Center, Sun Yat-Sen University, Guangzhou 510060, P.R. China; [2]Department of Neurosurgery, The First Affiliated Hospital of Sun Yat-Sen University, Guangzhou 510080, P.R. China; [3]Department of Stomatology, The First Affiliated Hospital of Sun Yat-Sen University, Guangzhou 510080, P.R. China. [*]Co-first authors.

Received October 14, 2018; Accepted June 10, 2019; Epub July 15, 2019; Published July 30, 2019

Abstract: A 20-year-old male sustained right fronto-orbito-temporal trauma, multiple skull fractures, and rupturing of the right eyeball in a motor vehicle collision. The patient underwent emergency right frontotemporal surgery for evacuation of a right intracranial hematoma, repair of the anterior skull base, decompressive craniectomy, and reduction and fixation of the right zygomatic arch. This was combined with debridement and suturing of the right-eye scleral rupture. At 10 months postsurgery, a defect measuring approximately 112.2 × 134.3 mm, along with a collapse affecting the right frontotemporal bone, right superciliary arch, orbital roof, and orbital lateral wall, remained. Angulation deformities of the right upper eyelid, eyeball atrophy, and absence of light perception were also observed. Computer-aided design (CAD) was employed to construct a three-dimensional (3D) skull model. This model was used to calculate the defect area and design the size and rim of a prosthesis, aiming to restore skull contour and enhance cosmetic appearance. Using computer-aided manufacturing (CAM), polyetheretherketone (PEEK) implants were cut, adjusted, packed, and sterilized. The skull implant, manufactured by CAD/CAM and 3D printing, perfectly fit the skull defect. Implantation surgery proceeded successfully, quickly, and conveniently. At the 5-month postoperative follow-up session, the patient reported no discomfort. Blood supply to the prosthesis surface was excellent. There was no dislocation observed between the implant and recipient skull. Enucleation and implantation of a hydroxyapatite artificial eye, in combination with eyelid reconstruction surgery, were then performed.

Keywords: CAD/CAM and 3D printing cranio-orbital defect

Case presentation

Collection and evaluation of protected patient health information was in compliance with the Health Insurance Portability and Accountability Act (HIPAA). In November 2014, a 20-year-old male was admitted to the Emergency Department of a local hospital after a car accident. He was in a coma for 1 hour. He was diagnosed with open craniofacial trauma, affecting the right frontal orbit, a comminuted skull fracture of the right side, brain contusion of the right fronto-temporal lobe and the left frontal lobe, and multiple fractures of the right orbit, ethmoid sinus, and maxillary sinus wall, as well as right eyeball rupturing and right eyelid lacerations (full-thickness layer). He subsequently underwent frontotemporal open surgery of the right orbit for evacuation of the intracranial hematoma, repair of the anterior skull base, decompressive craniectomy, and reduction and fixation of the right zygomatic arch, combined with debridement and suturing of the right eye scleral rupture. After 10 months of comprehensive function rehabilitation, limb and language function were restored. However, right-side frontal, temporal, and parietal bone defects, evident soft tissue collapses, and superciliary

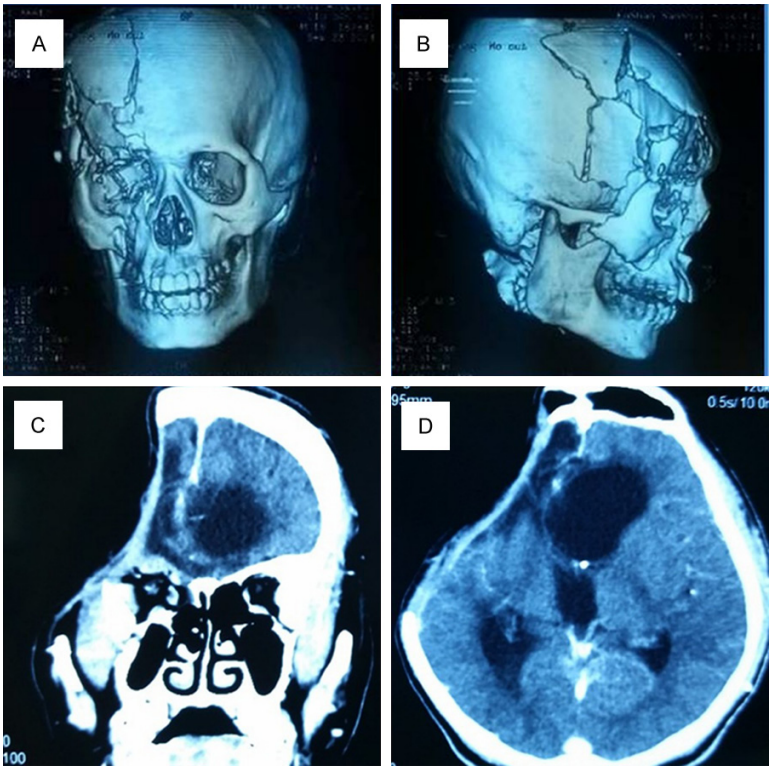

Figure 1. Presurgical condition. A, B. Emergency CT revealing multiple comminuted fractures affecting the skull, zygomatic, and orbital region; C, D. After a decompressive craniectomy for open frontal craniocerebral trauma of the right orbit, CTs revealed defects and a collapse of the right frontal, temporal, and parietal bone, defects affecting the superciliary arch, orbital roof, and orbital lateral wall, and soft tissue collapse.

arch, orbital roof, and orbital lateral wall defects and collapse (112.2 mm × 134.3 mm in size) were observed. In addition, he suffered from right upper eyelid angulation deformities, eyeball atrophy, and no light perception (**Figure 1**).

Written informed consent was obtained from the patient and family members. After rounds of multi-disciplinary consultations, CAD/CAM, in combination with 3D printing, was preliminarily chosen for the design and manufacture of a prosthesis, according to the following procedures. (1) Prior to surgery, high-resolution spiral CT (0.5 mm) and MRIs of the entire head were performed in the transverse, sagittal, and coronal planes, aiming to observe the repair of soft tissue and anatomical relationships of the bone defect region and surrounding bone and soft tissue; (2) CT scan data were input into Materialise's interactive medical image control system to construct a 3D model of the entire skull. The skull was printed at a 1:1 size ratio using a 3D printer. Hence, the surgeons and prosthesis manufacturers could directly observe the skull defect region; (3) The bone defect area was calculated via Mimics software using CAD. Fitting, curvature, and the rim of the prosthesis were designed. In this case, the skull defect area was large with irregular rims. To facilitate intraoperative implantation and decrease intraoperative injuries, the prosthesis was designed in two parts using CAD. One part extended from the fronto-superciliary arch and orbital roof to the lateral orbit. The other part consisted of the frontotemporal bone plate. The two parts were fitted with a dentate joint; (4) The bone plate implant was made from PEEK material. It was cut, burnished, polished, and processed by CAM; (5) After skull model printing, trial fixing was conducted to validate the curvature, rim, fitting, and symmetry of the prosthesis, as shown in **Figure 2**. Artificial adjustments were made according to the circumstances; (6) The bone plate implant was packed and sterilized in the operating room.

In September 2015, the patient underwent a frontotemporal cranioplasty procedure of the right superciliary arch, orbital roof, and orbital lateral wall under general anesthesia. Intraoperatively, scalp and galea aponeurotica incisions were created along the original surgical scars and supplementary mark lines. The skull flaps were separated under the galea aponeurotica. After the middle scar incision was created, the right frontotemporal flaps were shifted in superior-frontal and midline directions. The temporalis adhering to the dura mater surface was separated to expose the basilar bone window rim of the middle skull, lateral zygomatic process of the right orbit, and the bone rim of the basis frontalis midline. This fully exposed the upper and posterior rims of the bone window within the skull defect area. The anterior part (right fronto-superciliary arch,

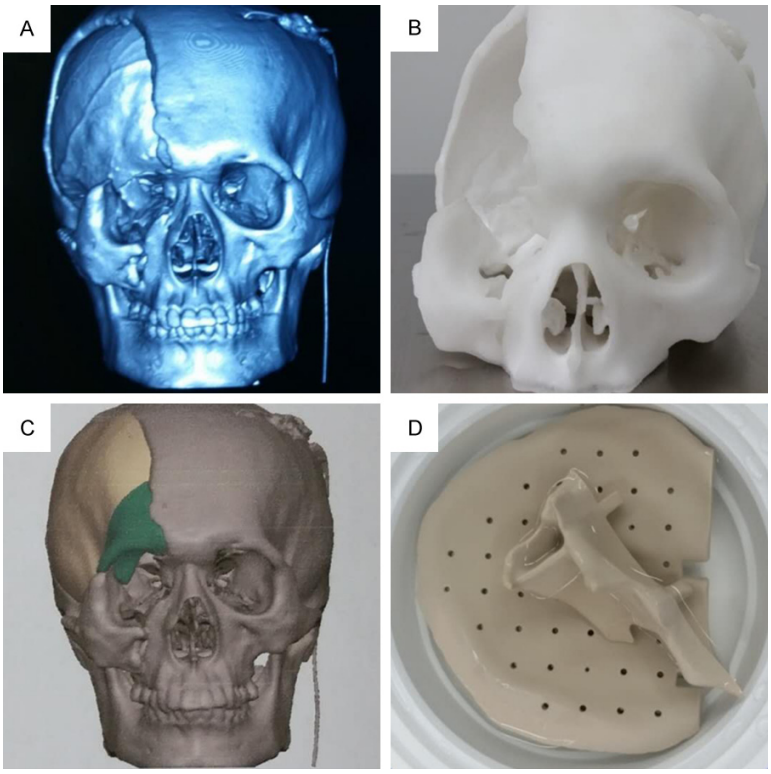

Figure 2. Computer-aided design and manufacturing strategy using 3D printing. A. 3D digitization simulation imaging of the head; B. 3D printing of that head model with a 1:1 aspect ratio; C. CAD simulation of the implant; D. Split prosthesis.

orbital roof, and lateral orbit) of the customized prosthesis was fixed to the original anatomical position using 4 pieces of 2-hole titanium strip. The posterior part was then fitted with the anterior part and fixed using the titanium strip. The dura mater was suspended and the remaining temporalis of the right side was sutured and fixed to the temporal surface of the implant. One piece of No.14 silicon rubber tube was placed under the scalp. Finally, the galea aponeurotica and scalp were sutured layer by layer. The prosthesis was successfully implanted and fixed.

The skull implant manufactured by CAD/CAM fit well with the skull defect model produced by 3D printing. Intraoperative and postoperative CTs and MRIs of the skull and orbit confirmed that the skull implant fit precisely with the bone defect region of the patient. In addition, the prosthesis was easily implanted in symmetry.

During the postoperative 5-month follow-up session, the patient reported no discomfort. The surface skin of the prosthesis had excellent blood supply and no dislocation was noted between the prosthesis and bone rim. CT re-examinations of the head and orbit confirmed that the prosthesis was symmetrical to the contralateral autologous skull and ossa orbitale. The rims were properly fitted. The prosthesis was surrounded by soft tissue and no edemas or tissue necrosis were documented. During the preliminary decompressive craniotomy procedure, the temporalis was utilized for repair of the midbrain membrane. Hence, a soft tissue defect was observed on the temporal side. A slight collapse of the temporal tissue was observed after mitigation of the tissue edema. Enucleation and implantation of a hydroxyapatite artificial eye (19 mm in diameter), along with eyelid reconstruction surgery, were then performed. No intraoperative indications were induced by the orbital prosthesis. The artificial eye was fixed accurately and stably. A favorable clinical outcome was obtained after surgery, as illustrated in **Figure 3**.

Discussion

Three-dimensional printing, also known as stereolithography, was developed by the Massachusetts Institute of Technology (MIT) in the 1990s as a rapid prototyping technique [1]. In additive manufacturing, 3D printing allows for the creation of objects of any composition, material, or geometric shape. Subsequently, 3D tissue printing was developed, allowing scientists to create liver, myocardium, tracheal stents, bionic ears, and blood vessels, as well as other tissues [2-5].

Conventional surgical repair of cranial orbital defects at multiple sites is challenging due to irregular rims, complex surface curvature, low plasticity of filling materials, and insufficient covering of subcutaneous soft tissues. Moreover, the narrow space and small visual field

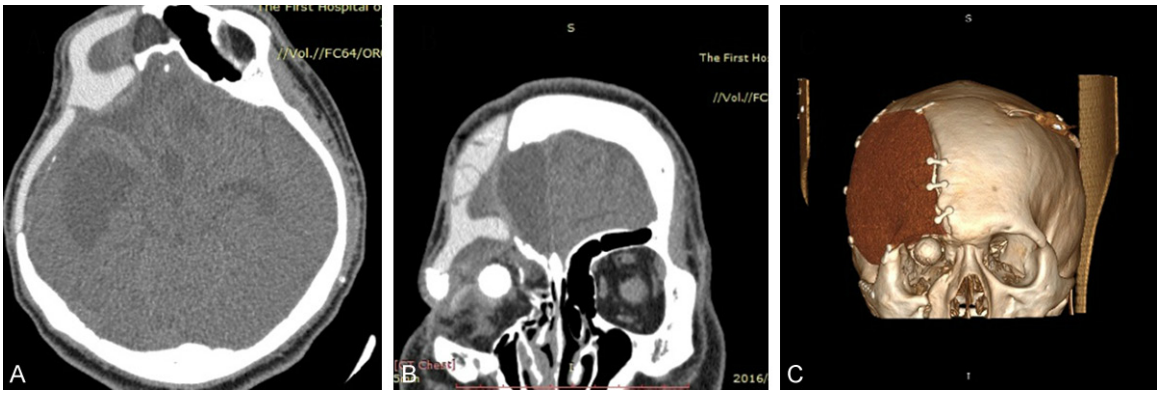

Figure 3. Surgical outcome. CT re-examination at 1 month after artificial eye implantation revealing that the (A-C) prosthesis was well fitted to the adjacent bone rims; (B, C) Artificial eye was stably placed with a high level of comfort and favorable cosmetic appearance.

Table 1. Comparison of density and thermal conductivity between different implant materials

Materials	Density (g × cm^{-3})	Thermal conductivity
Titanium alloy	4.4-4.5	16.3-18
Stainless steel	7.9	16.2
Hydroxyapatite	3.16	3.18-3.41
PEEK	1.30	0.25-0.92

during orbital surgery enhances surgical difficulty. Therefore, only experienced surgeons can successfully accomplish these procedures. Based on preoperative imaging findings, surgeons can roughly estimate the fracture location and parameters. Intraoperatively, surgeons have to manually adjust the shape, size, and rim of the prosthesis, according to their own clinical experience. This is both time- and energy-consuming. However, postoperative clinical efficacy may be poor, including unfavorable cosmetic appearance, bilateral asymmetry, poor rim fitting, and roughness of the overlap part. Furthermore, frequent placement and removal of the prosthesis also increases risks of infection. As 3D imaging and printing technologies have gradually matured, they have been widely applied in bone defect repairs, mainly in Orthopedics, Maxillofacial Surgery, and Neurosurgery. In recent years, researchers have applied 3D printing for repair of orbital defects [6].

Since 2016, the application scope of 3D printing has extended into the fields of plastic surgery, skull implantation, operative instruments, dental repair, and prosthesic limb surgery [7]. Using Materialise's interactive medical image control system (Mimics software), researchers can compile CT scan and MRI data to generate 3D images. Subsequently, 3D images are transferred through replicator G software. The object is printed with 1:1 size correspondence using a 3D printer. The model produced by the 3D printer can be used for preoperative observation, design of surgical procedures, assessment of surgical risk, design of prosthesis size and curvature, and surgical simulation, reducing the risk of surgical complications and enhancing the quality of medical treatment. Prior to surgery, most surgeons print and sterilize 3D models of the affected orbit and defect region. Intraoperatively, the rims of the prosthesis are cut to fit the defect region of the 3D model. According to the defect region of the 3D model, prosthesis implantation is simulated and the curvature of the prosthesis is adjusted [8, 9]. Although a patient-specific implant is produced and implantation times are shortened, this technology is not completely customized.

In the current study, CAD was utilized to simulate the contour and appearance of the defects. It was then used to create a skull model using 3D printing. During the process of prosthesis manufacturing, CAD/CAM was employed simultaneously. Based on geometric data from 3D computer graphics of the defects, blocks made from PEEK were cut, burnished, and polished, creating the initial prosthesis. The rims of the prosthesis were manually adjusted according to the defect window of the 3D-printed skull model, reducing the time required for rim cutting and risks of prolonged anesthesia.

Table 2. Comparison of mechanic parameters of different implant materials

Materials	Elastic modulus (GPa)	Bending strength (Mpa)	Fracture toughness (Mpa/m^2)
Titanium alloy	110-117	6758-1117	55-115
Stainless steel	189-205	170-310	50-200
Hydroxyapatite	73-117	600	0.7
PEEK	3.8-4.5	165	6.9
Human bone	3-20	130-180	3-6

Table 3. Comparison of infection rates between reconstruction materials after implantation

Materials	Range of infection rates in the literature(%)
Autograft	0-33
Allograft	0-9.5
PMMA (acrylic)	9.2-16
HA (hydroxyapatite)	0-20
Calcium phosphate	0-20
Porous polyethylene	0-5.6
Titanium mesh	0-2.3
Titanium PSI	0-6.7
PEEK	0 (no data available)

At present, this technology is applied for repair of orbital defects. This is primarily completed by Neurosurgery or Maxillofacial Surgery Department doctors [10-20]. In this report, the patient suffered from severe defects, involving the skull, zygoma, masseter, paries superior orbitae, upper lateral wall of the orbit, and frontal bone. Due to irregular surface defects and complex surgical procedures, diagnosis and treatment were determined by multi-disciplinary surgeons from the Department of Orthopedics, Department of Maxillofacial Surgery, and Department of Neurosurgery. Considering the deep and irregular defects in the orbit and orbital lateral wall, a split-implant consisting of two parts was designed in this case. This was opposed to previous studies in which one single implant was selected. One part of the split implant extended from the orbital rim and superior orbital wall to part of the frontal bone. The other part included the remaining frontal bone, zygoma, and parietal bone. These two parts were tightly connected by a dentate joint. The use of this split implant shortened the time required for placement, alleviating soft tissue injuries. Multiple postoperative CT scans revealed that the two parts were fitted properly. There was no sinking, dislocation, or bilateral asymmetry of the skull and orbital bones observed.

In addition to plasticity, the degree of comfort is another consideration when choosing implant materials. Despite excellent plasticity, titanium plates are highly sensitive to temperatures. Thus, dramatic temperature changes are likely to produce discomfort. Previous investigations have also demonstrated that titanium metal may cause thinning of soft tissue and extrusion of the implants [21]. Thus, PEEK was chosen as the manufacturing material for the implant. PEEK is a polymer material invented by the Victrex Corporation (UK) in 1978. It was later developed by the Invibio Corporation in the 1990s for medical use. In the decades since, PEEK has been widely applied for medical implant construction. It is now approved for medical use by the FDA, CE, CFDA, and PMDA. Most importantly, PEEK has mechanical characteristics highly similar to human bone [22]. Advantages of PEEK can be summarized as follows: (1) PEEK has moderate density, which is convenient for cutting, burnishing, and polishing. Thus, it can be precisely adjusted intraoperatively, as illustrated in **Table 1**; (2) PEEK is heat insulated and maintains a constant temperature. This reduces the risk of tissue tightening, headaches, and other discomforts caused by dramatic changes in ambient temperature (**Table 1**); (3) PEEK is an inert material with no magnetism. It does not interfere with imaging modalities. Thus, it is safe for MRIs and yields no artifacts. It also has favorable permeability characteristics for X-rays and high compatibility with CT imaging; (4) PEEK is lightweight, self-lubricating, and highly comfortable; and (5) PEEK elasticity and bending strength levels are similar to human bone. Thus, it can buffer collision and compression among tissues (**Table 2**). Recent studies have demonstrated that infection rates and incidence rates of rejection are extremely low using PEEK for craniofacial implants (**Table 3**). In addition, PEEK is characterized by stable physical properties, high-temperature resistance, and anti-acid and alkali erosion resistance. These allow for preparation for medical use after high temperature disinfection. However,

several limitations of PEEK should be acknowledged. Due to the smooth surface, PEEK is predominantly surrounded by cellulose after implantation and is resistant to vascularization. The high costs of PEEK also limit widespread application in hospital settings.

Several limitations of CAD/CAM, in combination with 3D printing, should also be acknowledged [23]: (1) Model manufacture depends completely on imaging data. Thus, small image flaws or measurement inaccuracies will impair fitting; (2) Standards of imaging equipment are demanding, including high-pixel CT with layer thickness < 1.5 mm or even ≤ 1 mm; (3) It is difficult to accurately reconstruct a 3D model and bone plate of the internal wall or deep orbital fracture, as well as defects, due to anatomic complexities. However, these limitations should be resolved by developments and advances in imaging technology; (4) Combined application of CAD/CAM and 3D printing requires the support of an industrialized manufacturing chain and mastery of computer digital technology by the surgeons. This is difficult to achieve at a single hospital level. In this report, both surgeons and imaging specialists participated in CAD, as well as the adjustment and processing of finished products. If the participants were not familiar with 3D reconstruction software, anatomical characteristics of the defect region, and the prosthesis manufacturing process, it would have been impossible to achieve perfect fitting between the prosthesis and human skull without an advanced manufacture chain; (5) Manufacturing and adjustments of 3D models and prostheses require 1 to 2 weeks. Thus, this methodology is not applicable in the Emergency Department; (6) In the current case, the prosthesis cost approximately 90,000 RMB (approximately 14,000 U.S. dollars). This is significantly more expensive than a conventional prosthesis, limiting widespread application, especially in developing countries.

In summary, combined application of CAD/CAM and 3D printing is an individualized approach for reconstruction of severe craniofacial and orbital defects. This method yields precise fitting, significantly improving cosmetic appearance. Prostheses composed of PEEK have multiple advantages, including imaging compatibility, heat resistance, temperature insensitivity, and self-lubrication. These advantages result in a high level of comfort. In addition, PEEK has mechanical properties very similar to human bone. Due to recent advances in computer science and biomaterial medicine, CAD/CAM, in combination with 3D printing, is more precise and cost-effective than in the past. Therefore, it confers clinical benefits to more patients in a wider range of clinical fields.

Acknowledgements

This work was supported by grants from the National Natural Science Foundation of China [81400384, 81570839].

Disclosure of conflict of interest

None.

Address correspondence to: Zhenhua Yu, Department of Neurosurgery, The First Affiliated Hospital of Sun Yat-Sen University, Guangzhou 510080, P.R. China. E-mail: yuzhenhua08@126.com; Yongxin Zheng, Department of Ocular Trauma, Zhong Shan Ophthalmic Center, Sun Yat-Sen University, Guangzhou 510060, P.R. China. E-mail: fdhqs@126.com

References

[1] Gross BC, Erkal JL, Lockwood SY, Chen C and Spence DM. Evaluation of 3D printing and its potential impact on biotechnology and the chemical sciences. Anal Chem 2014; 86: 3240-3253.

[2] Schubert C, van Langeveld MC and Donoso LA. Innovations in 3D printing: a 3D overview from optics to organs. Br J Ophthalmol 2014; 98: 159-161.

[3] Zopf DA, Hollister SJ, Nelson ME, Ohye RG and Green GE. Bioresorbable airway splint created with a three-dimensional printer. N Engl J Med 2013; 368: 2043-2045.

[4] Mannoor MS, Jiang Z, James T, Kong YL, Malatesta KA, Soboyejo WO, Verma N, Gracias DH and McAlpine MC. 3D printed bionic ears. Nano Lett 2013; 13: 2634-2639.

[5] Miller JS, Stevens KR, Yang MT, Baker BM, Nguyen DH, Cohen DM, Toro E, Chen AA, Galie PA, Yu X, Chaturvedi R, Bhatia SN and Chen CS. Rapid casting of patterned vascular networks for perfusable engineered three-dimensional tissues. Nat Mater 2012; 11: 768-774.

[6] Administration FaD. Additive manufacturing of medical devices: an interactive discussion on the technical considerations of 3D printing. 2014; 25.

[7] Administration FaD. Technical considerations for additive manufactured devices draft guidance until august 8, 2016. 2016; 28.

[8] Zhang H, Chen M, Li HM, Wang, Chai GR and Liu L. Application of 3D printer in making indi-

vidual orbital model. Chin J Ocul Traum Occupat Eye Dis 2015; 37: 5.
[9] Zheng SS, Bu ZY and Chai C. Application of computer-aided designing and manufacturing technology in the reconstruction of orbital blowout fracture. Chin J Exp Ophthalmol 2015; 33: 6.
[10] Martelli N, Serrano C, van den Brink H, Pineau J, Prognon P, Borget I and El Batti S. Advantages and disadvantages of 3-dimensional printing in surgery: a systematic review. Surgery 2016; 159: 1485-1500.
[11] Kim MM, Boahene KD and Byrne PJ. Use of customized polyetheretherketone (PEEK) implants in the reconstruction of complex maxillofacial defects. Arch Facial Plast Surg 2009; 11: 53-57.
[12] Hanasono MM, Goel N and DeMonte F. Calvarial reconstruction with polyetheretherketone implants. Ann Plast Surg 2009; 62: 653-655.
[13] Chacon-Moya E, Gallegos-Hernandez JF, Pina-Cabrales S, Cohn-Zurita F and Gone-Fernandez A. Cranial vault reconstruction using computer-designed polyetheretherketone (PEEK) implant: case report. Cir Cir 2009; 77: 437-440.
[14] Lai JB, Sittitavornwong S and Waite PD. Computer-assisted designed and computer-assisted manufactured polyetheretherketone prosthesis for complex fronto-orbito-temporal defect. J Oral Maxillofac Surg 2011; 69: 1175-1180.
[15] Camarini ET, Tomeh JK, Dias RR and da Silva EJ. Reconstruction of frontal bone using specific implant polyether-ether-ketone. J Craniofac Surg 2011; 22: 2205-2207.
[16] Scolozzi P. Maxillofacial reconstruction using polyetheretherketone patient-specific implants by "mirroring" computational planning. Aesthetic Plast Surg 2012; 36: 660-665.
[17] Goodson ML, Farr D, Keith D and Banks RJ. Use of two-piece polyetheretherketone (PEEK) implants in orbitozygomatic reconstruction. Br J Oral Maxillofac Surg 2012; 50: 268-269.
[18] Jalbert F, Boetto S, Nadon F, Lauwers F, Schmidt E and Lopez R. One-step primary reconstruction for complex craniofacial resection with PEEK custom-made implants. J Craniomaxillofac Surg 2014; 42: 141-148.
[19] Wang GL, Gong FH, Liu JL and Deng YF. Individualized reconstructive surgery for skull defects with poly-ether-ether-ketone materials. Chinese Journal of Minimally Invasive Neurosurgery 2013; 18: 3.
[20] Coulter C, Richards R, Peterson D, Collier J. Parietal skull reconstruction using immediate peek cranioplasty following resection for craniofacial fibrous dysplasia. J Plast Reconstr Aesthet Surg 2014; 67: e208-e209.
[21] Thien A, King NK, Ang BT, Wang E and Ng I. Comparison of polyetheretherketone and titanium cranioplasty after decompressive craniectomy. World Neurosurg 2015; 83: 176-180.
[22] Lethaus B, Safi Y, ter Laak-Poort M, Kloss-Brandstatter A, Banki F, Robbenmenke C, Steinseifer U and Kessler P. Cranioplasty with customized titanium and PEEK implants in a mechanical stress model. J Neurotrauma 2012; 29: 1077-1083.
[23] Neovius E and Engstrand T. Craniofacial reconstruction with bone and biomaterials: review over the last 11 years. J Plast Reconstr Aesthet Surg 2010; 63: 1615-1623.